

PV Cell Fed High Voltage Gain Coupled Inductor Based Input Parallel Output Series DC-DC Converter for Grid Connected System

Srinu Banavath

M-tech Student Scholar

Department of Electrical & Electronics Engineering,
 Nova College of Engineering and Technology, Jupudi,
 Ibrahimpatnam, Krishna District, AP, India
 Email: srinubanavath4547@gmail.com.

Lella.Veeru Kotlu

Associate Professor

Department of Electrical & Electronics Engineering,
 Nova College of Engineering and Technology, Jupudi,
 Ibrahimpatnam, Krishna District, AP, India
 Email: veeru.lella@gmail.com.

Abstract- Solar energy is the most low cost, competition free, universal source of energy as sun shines throughout. This energy can be converted into useful electrical energy using photovoltaic technology. Photovoltaic technology is one of the most promising for distributed low-power electrical generation. Converting the sun's radiation directly into electricity is done by solar cells. These cells are made of semiconducting materials similar to those used in computer chips. Photovoltaic arrays may operate more or less efficiently, depending on their series/parallel configuration. Converters like Buck, Boost and Buck-Boost converters are popularly used for photovoltaic systems. But these converters are limited to low power applications. For PV applications like pumping these converters could do a good job as pumping is carried out at high power. Presently dc-dc converters are required in many industrial applications, to improve the voltage. The grid connected DC-DC converters are used for low input-voltage and high step up power conversion, this paper has successfully developed a high-voltage gain dc-dc converter by input-parallel output-series and inductor techniques. In this paper a novel input-parallel output-series boost converter with dual coupled inductors and a voltage multiplier module. The simulation results are presented by using Matlab/simulink software.

Key words- PV system, dc-dc converter, dual coupled output

1. INTRODUCTION

At the threshold of opportunity to grow India has expanded its role in PV adoption and manufacturing. Recently the use of step-up DC-DC converters with high voltage ratio has been increased. That is due to the growing usage of this type of converters in a wide range of applications such as fuel cell stacks (FC), photovoltaic (PV) cells, uninterruptable power supplies (UPS), etc. [1]-[4]. The major problems of PV system is that the output voltage of PV panels is highly dependent on solar irradiance and ambient temperature. Unfortunately, once there is a partial shadow on some panels, the systems energy yields becomes significantly reduced [5]. Hence loads cannot be connected directly to the output PV panels. In these sorts of applications high step-up converters are used to convert the low level varying primary voltage to the desired regulated high voltage output.

The main drawbacks of PV energy is the high cost of silicon solar panels and low conversion efficiency. Some latest technologies like the use of crystalline panels and effective power converter design, it is possible to make a PV paper cost effective. Also the conversion of the output voltage from a solar panel into usable DC or AC voltage can be done at its maximum power point, or MPP. MPP is the PV output voltage at which the module delivers maximum energy to load [6-7].

Another method for achieving high step-up gain is the use of the voltage-lift technique, showing the advantage that the voltage stress across the switch is low. However, several diode-capacitor stages are required when the conversion ratio is very large, which makes the circuit complex. In addition, the single switch may suffer high current for high power applications, which risks reducing its efficiency [8-9]. Another alternative single switch converters including forward, fly-back and tapped-inductor boost can achieve high conversion ratio by adjusting the turns ratio of the transformer, but these converters require large transformer turns ratio to achieve high voltage gain. In, an integrated boost-fly back converter is proposed to achieve high voltage gain, and the energy of a leakage inductor is recycled into the output during the switch-off period. Unfortunately, the input current is pulsed from the experimental results. In addition, it should be noticed that the low-level input voltages usually cause large input currents and current ripples to flow through the single switch for high step up and high power DC-DC conversion, which also leads to increasing conduction losses [10-12].

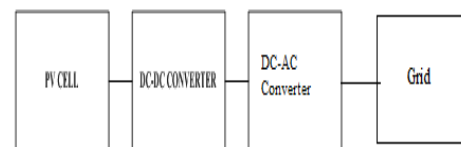


Fig.1.Block diagram

(A) DC-DC CONVERTER

Nowadays high voltage gain DC-DC converters are required in many industrial applications. Photovoltaic

energy conversion systems and fuel-cell systems usually need high step up and large input current dc-dc converters to boost low voltage (18-56 V) to high voltage (200-400 V) for the grid-connected inverters. High-intensity discharge lamp ballasts for automobile headlamps call for high voltage gain DC-DC converters to raise a battery voltage of 12 V up to 100 V at steady operation. Also, the low battery voltage of 48 V needs to be converted to 380 V in the front-end stage in some uninterruptible power supplies and telecommunication systems by high step-up converters. Theoretically, a basic boost converter can provide infinite voltage gain with extremely high duty ratio. In practice, the voltage gain is limited by the parasitic elements of the power devices, inductor and capacitor. Moreover, the extremely high duty cycle operation may induce serious reverse-recovery problem of the rectifier diode and large current ripples, which increase the conduction losses. On the other hand, the input current is usually large in high output voltage and high power conversion, but low-voltage-rated power devices with small on resistances may not be selected since the voltage stress of the main switch and diode is, respectively, equivalent to the output voltage in the conventional boost converter. Many other converter topologies have developed for high step up gain. Here a high gain input-parallel output-series DC-DC converter with dual coupled inductors is designed. This configuration inherits the merits of high voltage gain, low output voltage ripple, and low voltage stress across the power switches. Moreover, the converter is able to turn ON the active switches at zero current and alleviate the reverse recovery problem of diodes by reasonable leakage inductances of the coupled inductors [11-12].

(B) Photovoltaic system

A photovoltaic system, also solar PV power system, or PV system, is a power system designed to supply usable solar power by means of photovoltaic. It consists of an arrangement of several components, including solar panels to absorb and convert sunlight into electricity, a solar inverter to change the electric current from DC to AC, as well as mounting, cabling and other electrical accessories to set up a working system. It may also use a solar tracking system to improve the system's overall performance and include an integrated battery solution, as prices for storage devices are expected to decline. Strictly speaking, a solar array only encompasses the ensemble of solar panels, the visible part of the PV system, and does not include all the other hardware, often summarized as balance of system (BOS). Moreover, PV systems convert light directly into electricity and shouldn't be confused with other technologies, such as concentrated solar power or solar thermal, used for heating and cooling. PV systems range from small, rooftop-mounted or building-integrated systems with capacities from a few to several tens of kilowatts, to large utility-scale power stations of hundreds of megawatts. Nowadays, most PV

systems are grid-connected, while off-grid or stand-alone systems only account for a small portion of the market. Operating silently and without any moving parts or environmental emissions, PV systems have developed from being niche market applications into a mature technology used for mainstream electricity generation. A rooftop system recoups the invested energy for its manufacturing and installation within 0.7 to 2 years and produces about 95 percent of net clean renewable energy over a 30-year service lifetime.[1]

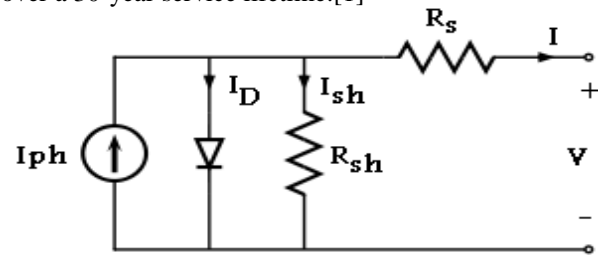


Fig 2. PV cell equivalent circuit.

Figure reflects a simple equivalent circuit of a photovoltaic cell. The current source which is driven by sunlight is connected with a real diode in parallel. In this case, PV cell presents a p-n junction characteristic of the real diode. The forward current could flow through the diode from p-side to n-side with little loss. However, if the current flows in reverse direction, only little reverse saturation current could get through.

Due to the exponential growth of photovoltaic, prices for PV systems have rapidly declined in recent years. However, they vary by market and the size of the system. In 2014, prices for residential 5-kilowatt systems in the United States were around \$3.29 per watt,[4] while in the highly penetrated German market, prices for rooftop systems of up to 100 kW declined to €1.24 per watt.[5] Nowadays, solar PV modules account for less than half of the system's overall cost,[6] leaving the rest to the remaining BOS-components and to soft costs, which include customer acquisition, permitting, inspection and interconnection, installation labor and financing costs

II. TOPOLOGY AND OPERATION PRINCIPLE OF THE PRESENTED CONVERTER

The derivation procedure for the proposed topology is shown in Fig.3. This circuit can be divided as two parts. These two segments are named a modified interleaved boost converter and a voltage doubler module using capacitor–diode and coupled inductor technologies. The basic boost converter topology shown in Fig. 3.(a) and (b) is another boost version with the same function in which the output diode is placed on the negative dc-link rail. Fig. 3(c) is called a modified interleaved boost converter, which is an input-parallel and output-series configuration derived from two basic boost types. Therefore, this part based on interleaved control has several main functions: 1) it can obtain double voltage gain of the conventional

interleaved boost; 2) low output voltage ripple due to the interleaved series connected capacitors; and 3) low switch voltage stresses. Then, the double independent inductors in the modified interleaved boost converter are separately replaced by the primary windings of coupled inductors that are employed as energy storage and filtering as shown in Fig.3 (d). The secondary windings of two coupled inductors are connected in series for a voltage multiplier module, which is stacked on the output of the modified converter to get higher voltage gain. Fortunately, this connection is also helpful to balance the currents of two primary sides. The coupling references of the inductors are denoted by the marks “*” and “.”. The equivalent circuit of the presented converter is demonstrated. Where:

- 1) L_{m1} , L_{m2} : magnetizing inductances;
- 2) L_{k1} , L_{k2} : leakage inductances;
- 3) C_1 , C_2 , C_3 : output and clamp capacitors;
- 4) S_1 , S_2 : main switches;
- 5) D_1 , D_2 : clamp diodes;
- 6) D_r , C_r : regenerative diode and capacitor;
- 7) D_3 : output diode;
- 8) N : turns ratio of N_s/N_p ;
- 9) V_{N1} , V_{N2} : the voltage on the primary sides of coupled inductors

Fig. 3. shows the theoretical waveforms when the converter is operated in continuous conduction mode (CCM). The duty cycles of the power switches are interleaved with 180° phase shift, and the duty cycles are greater than 0.5. That is to say, the two switches can only be in one of three states (S_1 : ON, S_2 : ON; S_1 : ON, S_2 : OFF; S_1 : OFF, S_2 : ON), which ensures the normal transmission of energy from the coupled inductor's primary side to the secondary one. The operating stages can be found in Fig.4.

1).First stage [t_0-t_1]: At $t = t_0$, the power switch S_1 is turned on with zero-current switching (ZCS) due to the leakage inductance L_{k1} , while S_2 remains turned ON, as shown in Fig. 4. Diodes D_1, D_2 , and D_r are turned OFF, and only output diode D_3 is conducting. The current falling rate through the output diode D_3 is controlled by the leakage inductances L_{k1} and L_{k2} , which alleviates the diodes' reverse recovery problem. This stage ends when the current through the diode D_3 decreases to zero.

2).Second stage [t_1-t_2]: During this interval, both the power switches S_1 and S_2 are maintained turned ON, as shown in Fig.5 All of the diodes are reversed-biased. The magnetizing inductances L_{m1} and L_{m2} as well as leakage inductances L_{k1} and L_{k2} are linearly charged by the input voltage source V_{in} . This period ends at the instant t_2 , when the switch S_2 is turned OFF.

3) Third stage [t_2-t_3]: At $t = t_2$, the switch S_2 is turned OFF, which makes the diodes D_2 and D_r turned ON. The current flow path is shown in Fig.6. The energy that magnetizing inductance L_{m2} has stored is transferred to the secondary side charging the capacitor C_r by the diode

D_r , and the current through the diode D_r and the capacitor C_r is determined by the leakage inductances L_{k1} and L_{k2} . The input voltage source, magnetizing inductance L_{m2} and leakage inductance L_{k2} release energy to the capacitor C_2 via diode D_2 .

4) Fourth stage [t_3-t_4]: At $t = t_3$, diode D_2 automatically switches OFF because the total energy of leakage inductance L_{k2} has been completely released to the capacitor C_2 . There is no reverse recovery problem for the diode D_2 . The current-flow path of this stage is shown in Fig.7. Magnetizing inductance L_{m2} still transfers energy to the secondary side charging the capacitor C_r via diode D_r . The current of the switch S_1 is equal to the summation of the currents of the magnetizing inductances L_{m1} and L_{m2} .

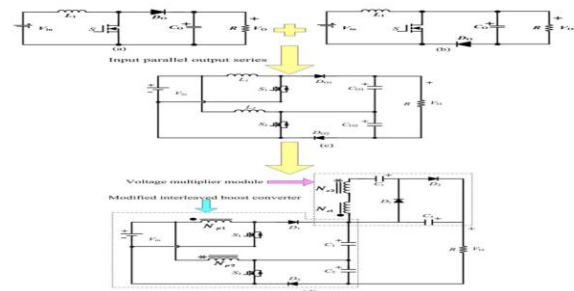


Fig. 3. Procedure to obtain the proposed converter with high voltage gain. (a) Conventional boost converter. (b) Other structure of boost converter. (c) Modified interleaved boost. (d) High gain input-parallel output-series dc/dc converter with dual coupled inductors.

5).Fifth stage [t_4-t_5]: At $t = t_4$, the switch S_2 is turned ON with ZCS soft-switching condition. Due to the leakage inductance L_{k2} and the switch S_1 remains in ON state. The current flow path of this stage is shown in Fig. 8. The current falling rate through the diode D_r is controlled by the leakage inductances L_{k1} and L_{k2} , which alleviates the diode reverse recovery problem. This stage ends when the current through the diode D_r decreases to zero at $t = t_5$.

6).Sixth stage [t_5-t_6]: The operating states of stages 6 and 2 are similar. During this interval, all diodes are turned OFF. The magnetizing inductances L_{m1} and L_{m2} , and the leakage inductances L_{k1} and L_{k2} are charged linearly by the input voltage. The voltage stress of D_1 is the voltage on C_1 , and the voltage stress of D_2 is the voltage on C_2 . The voltage stress of D_r is equivalent to the voltage on C_r , and the voltage stress of D_3 is the output voltage minus the voltages on C_1 and C_2 and C_r .

7).Seventh stage [t_6-t_7]: The power switch S_1 is turned OFF at $t = t_6$, which turns ON D_1 and D_3 , and the switch S_2 remains in conducting state. The current-flow path of this stage is shown in Fig. 10. The input voltage source V_{in} , magnetizing inductance L_{m1} and leakage inductance L_{k1} release their energy to the capacitor C_1 via the switch S_2 . Simultaneously, the energy stored in magnetizing inductor L_{m1} is transferred to the secondary side. The

current through the secondary sides in series flows to the capacitor C3 and load through the diode D3.

8. Eighth stage [t7-t0]: At t = t7, since the total energy of leakage inductance Lk1 has been completely released to the capacitor C1, diode D1 automatically switches OFF. The current of the magnetizing inductance Lm1 is directly transferred to the output through the secondary side of coupled inductor and D4 until t'0.

It should be pointed out that the time periods of stages I, IV, V, and VIII are much shorter than those shown in Fig. 3., which were enlarged in order to clearly show the waveform variations.

III. STEADY-STATE PERFORMANCE ANALYSIS OF THE PROPOSED CONVERTER

To simplify the circuit performance analysis of the proposed converter in CCM, the following conditions are assumed.

- 1) All of the power devices are ideal. That is to say, the on-state resistance RDS (ON) and all parasitic capacitors of the main switches are neglected, and the forward voltage drop of the diodes is ignored.
- 2) The coupling-coefficient k of each coupled inductor is defined as $L_m / (L_m + L_k)$. The turn ratio N of each coupled inductor is equal to N_s / N_p .
- 3) The parameters of two coupled inductors are considered to be the same, namely $L_{m1} = L_{m2} = L_m$, $L_{k1} = L_{k2} = L_k$, $N_{s1} / N_{p1} = N_{s2} / N_{p2} = N$, and $k_1 = L_{m1} / (L_{m1} + L_{k1}) = k_2 = L_{m2} / (L_{m2} + L_{k2}) = k$.
- 4) Capacitors C1, C2, C3, and Cr are large enough. Thus, the voltages across these capacitors are considered as constant in one switching period.

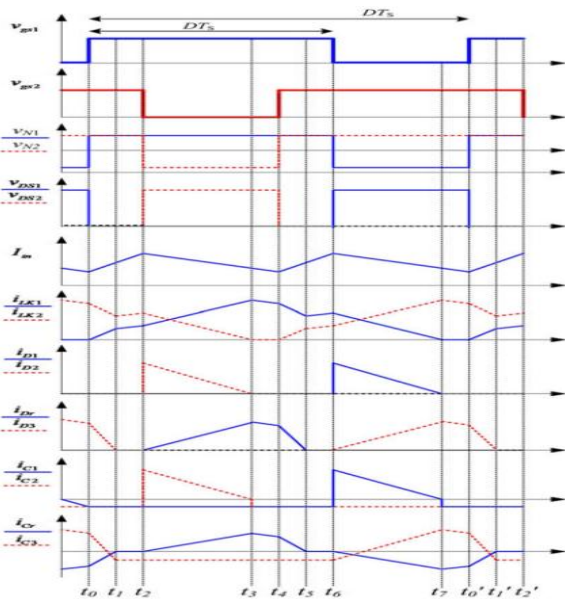


Fig. 4. Key theoretical waveforms.

(A) Voltage Gain Expression

If the transient characteristics of circuit are disregarded, each magnetizing inductance has two main states in one switching period. In one state, the magnetizing inductance is charged by the input source. In the other state, the magnetizing inductance is discharged by the output capacitor voltage VC 1 or VC 2 minus the input voltage. Since the time durations of stages I, IV, V, and VIII are significantly short, only stages II, III, VI, and VII are considered for the steady-state analysis. At stages II and VI, the

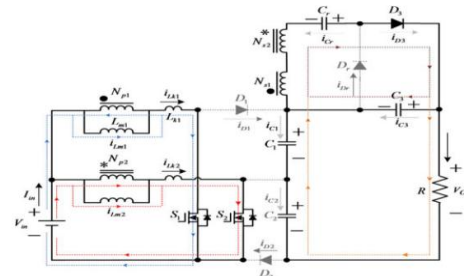


Fig.5. First stage

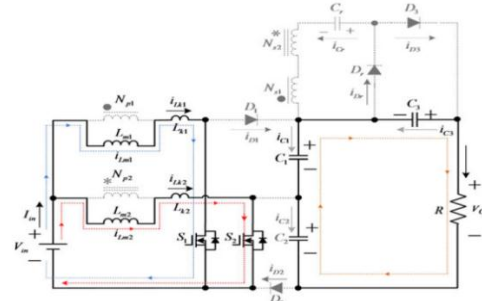


Fig.6. Second stage

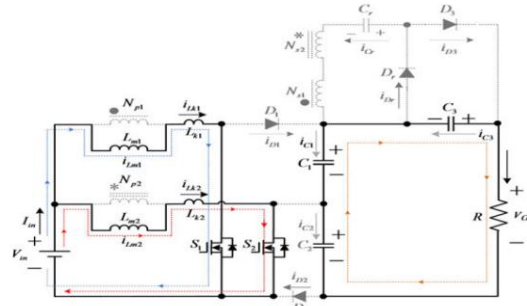


Fig.7. Second stage

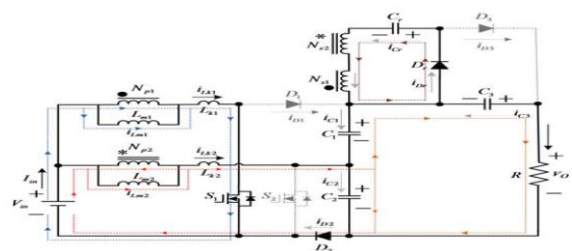


Fig.8. Third stage.

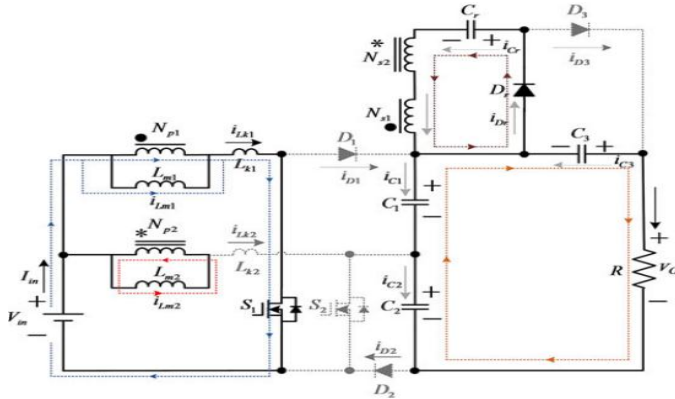


Fig. 9. Fourth stage

Following equations can be written from Figs.5 and 9

$$V_{Lm1}^{II} = V_{Lm1}^{VI} = kV_{in} \quad (1)$$

$$V_{Lm2}^{II} = V_{Lm2}^{VI} = kV_{in} \quad (2)$$

$$V_o = V_{C1} + V_{C2} + V_{C3} \quad (3)$$

At stage III, the following equations are derived from Fig.6:

$$V_{Lm1}^{III} = kV_{in} \quad (4)$$

$$V_{Lm2}^{III} = k(V_{in} - V_{C2}) \quad (5)$$

$$V_{Cr} = V_{S1} - V_{S2} = kNV_{C2} \quad (6)$$

During the time duration of stage VII, the following voltage equations can be expressed based on Fig. 10:

$$V_{Lm1}^{VII} = k(V_{in} - V_{C1}) \quad (7)$$

$$V_{Lm2}^{VII} = kV_{in} \quad (8)$$

$$V_{C3} = V_{Cr} + V_{S2} - V_{S1} = kN(V_{C1} + V_{C2}) \quad (9)$$

Using the volt-second balance principle on Lm1 and Lm2, respectively, the following equation is derived:

$$\int_0^{\frac{(2D-1)T}{2}} V_{Lm1}^{II} dt + \int_0^{(1-D)T} V_{Lm1}^{III} dt + \int_0^{\frac{(2D-1)T}{2}} V_{Lm1}^{VI} dt + \int_0^{(1-D)T} V_{Lm1}^{VII} dt = 0 \quad (10)$$

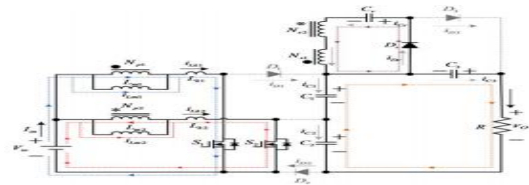


Fig.10. Fifth stage.

IV. MATLAB/SIMULATION RESULTS

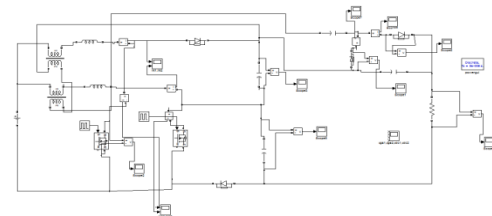


Fig. 11. Matlab/simulation circuit of High Step-up Input-Parallel Output-Series DC/DC Converter with Dual Coupled Inductors.

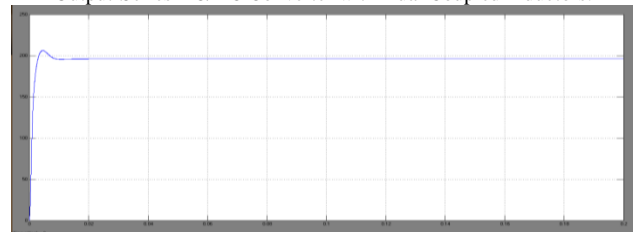


Fig 12 simulation wave form output voltage.

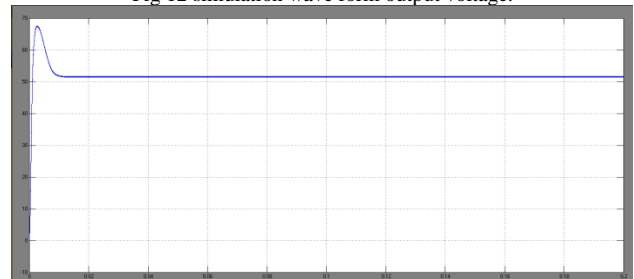


Fig 13 simulation wave form couple of inductance voltage.

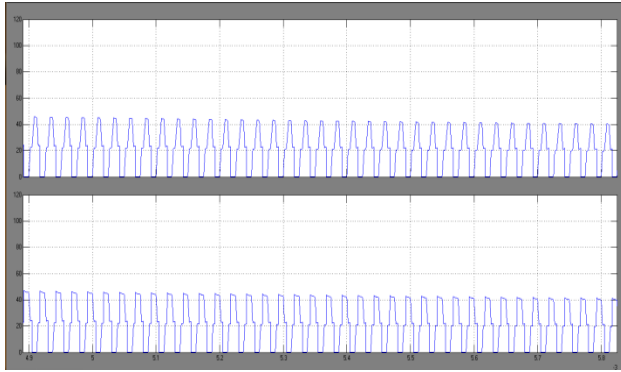


Fig 14 simulation wave form couple of inductance current.

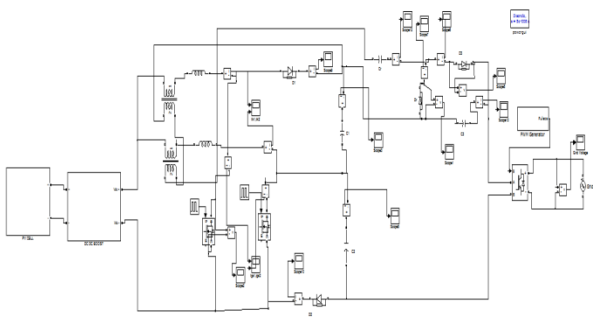


Fig 15 Matlab/simulation circuit of High Step-up Input-Parallel Output-Series DC/DC Converter with Dual Coupled Inductors with PV

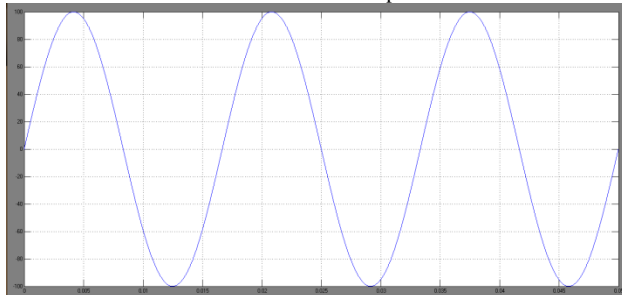


Fig 16 simulation wave form of High Step-up Input-Parallel Output-Series DC/DC Converter with Dual Coupled Inductors with PV output voltage

V. CONCLUSION

Low input voltage and high energy step changes, this paper successfully developed and series' inductor production volumes and parallel input techniques as high-voltage Converter has been achieved. The proposed dc converter is simple in construction and has more efficiency than the conventional dc-dc converter. This can be used in battery operated vehicles, and solar powered uninterrupted power supplies and can have significant use in renewable energy sources where there is a need of efficient dc conversion. The key theoretical waveforms, steady-state operational principle, and the main circuit performance are discussed to explore the advantages of the proposed converter. Performance of the converter is simulated using MATLAB/SIMULINK software.

REFERENCES

[1] C. Cecati, F. Ciancetta, and P. Siano, "A multilevel inverter for photovoltaic systems with fuzzy logic control," *IEEE Trans. Ind. Electron.*, vol. 57, no. 12, pp. 4115–4125, Dec. 2010.

[2] X. H. Yu, C. Cecati, T. Dillon, and M. G. Simoes, "The new frontier of smart grid," *IEEE Trans. Ind. Electron. Mag.*, vol. 15, no. 3, pp. 49–63, Sep. 2011.

[3] G. Fontes, C. Turpin, S. Astier, and T. A. Meynard, "Interactions between fuel cell and power converters: Influence of current harmonics on a fuel cell stack," *IEEE Trans. Power Electron.*, vol. 22, no. 2, pp. 670–678, Mar. 2007.

[4] J. Y. Lee and S. N. Hwang, "Non-isolated high-gain boost converter using voltage-stacking cell," *Electron. Lett.*, vol. 44, no. 10, pp. 644–645, May 2008.

[5] Z. Amjadi and S. S. Williamson, "Power-electronics-based solutions for plug-in hybrid electric vehicle energy storage and management systems," *IEEE Trans. Ind. Electron.*, vol. 57, no. 2, pp. 608–616, Feb. 2010.

[6] L. Henrique, S. C. Barreto, P. P. Praca, D. S. Oliveira Jr., and R. N. A. L. Silva, "High-voltage gain boost converter based on three-state commutation cell for battery charging using PV panels in a single conversion stage," *IEEE Trans. Power Electron.*, vol. 29, no. 1, pp. 150–158, Jan. 2014.

[7] F. Boico, B. Lehman, and K. Shujaee, "Solar battery chargers for NiMH batteries," *IEEE Trans. Power Electron.*, vol. 22, no. 5, pp. 1600–1609, Sep. 2007.

[8] A. Reatti, "Low-cost high power-density electronic ballast for automotive HID lamp," *IEEE Trans. Power Electron.*, vol. 15, no. 2, pp. 361–368, Mar. 2000.

[9] A. I. Bratcu, I. Munteanu, S. Bacha, D. Picault, and B. Raison, "Cascaded DC-DC converter photovoltaic systems: Power optimization issues," *IEEE Trans. Ind. Electron.*, vol. 58, no. 2, pp. 403–411, Feb. 2011.

[10] H. Tao, J. L. Duarte, and M. A. M. Hendrix, "Line-interactive UPS using a fuel cell as the primary source," *IEEE Trans. Ind. Electron.*, vol. 55, no. 8, pp. 3012–3021, Aug. 2008.

[11] Y. P. Hsieh, J. F. Chen, T. J. Liang, and L. S. Yang, "Novel high step-up DC-DC converter for distributed generation system," *IEEE Trans. Ind. Electron.*, vol. 60, no. 4, pp. 1473–1482, Apr. 2013.

[12] M. H. Todorovic, L. Palma, and P. N. Enjeti, "Design of a wide input range dc-dc converter with a robust power control scheme suitable for fuel cell power conversion," *IEEE Trans. Ind. Electron.*, vol. 55, no. 3, pp. 1247–1255, Mar. 2008.